Scientific Journal of Impact Factor (SJIF): 4.72

e-ISSN : 2348-4470
p-ISSN : 2348-6406

International Journal of Advance Engineering and Research Development

National Conference On Nanomaterials, (NCN-2017)

Volume 4, Special Issue 6, Dec.-2017 (UGC Approved)

Photoluminescence of Reactive Plasma Synthesized ZrO_2 Nanoparticles

S. Jayakumar*[1], K. Senthil kumaran[2,3], J.Poongkothai[4] , G.K.D. Prasanna venkatesan[5]

[1]*Assistant professor, Department of Physics, SNS College of Engineering, Coimbatore – 641107, India*
[2,]*Assistant professor, Department of Chemistry, SNS College of Engineering, Coimbatore – 641107, India*
[3]*Research Scholar, Research and Development Centre, Bharathiar University, Coimbatore – 641046, India*
[4]*Assistant professor, Department of Mathematics, Government Arts College, Udumalpet – 642126, India*
[5]*Professor, Department of Electronics and Communication, SNS College of Engineering, Coimbatore – 641107, India*

Abstract: *Pure ZrO_2 is reported to exhibit photoluminescence in different wavelengths of UV and visible region. This observed luminescence is related to defects and /or impurities in the system. The luminescent properties of ZrO_2, also depend strongly on the preparation methods. Though few works on optical properties of ZrO_2 were reported no detailed luminescence mechanisms were proposed. The present work investigates photoluminescence properties of reactive plasma synthesized ZrO_2 as a function of annealing temperature, time and annealing atmosphere. The as synthesized ZrO_2 contains mixture of tetragonal and monoclinic phase with crystallite size 15 nm and 25 nm respectively. The UV – visible absorption studies of the sample demonstrated two absorption bands at 3.94 and 4.5 eV which are lower than the band gap of ZrO_2. This narrowing of band gap was attributed to the oxygen vacancy levels developed in the band gap ZrO_2. Photoluminescence spectra of ZrO_2 sample showed two emission bands at 325 and 470 nm independent of excitation wavelengths. According to the emission-intensity dependence on the annealing atmospheres, it was proposed that the 325 nm band and the 470 nm band originate from F^+ centers and AOD^+ centers, respectively.*

Keywords: *ZrO_2, Plasma Processing, Nanoparticle, photoluminescence*

1. Introduction

Zirconia and Zirconia-based ceramics have been used as catalysts, oxygen sensors, high dielectric constant materials for very large scale integrated circuits, solid state electrolytes, thermal barrier coatings, electro-optical materials and as gate dielectrics in metal oxide-semiconductor devices [1 - 5]. Zirconia (ZrO_2) exhibits three crystallographic polymorphs with increasing temperature at ambient pressure: the monoclinic phase, from room temperature to 1175 °C; the tetragonal phase, from 1175 to 2370 °C; and the cubic phase, from 2370 to 2750 °C [6]. The mechanical, electric, catalytic and thermal properties of ZrO_2 have been well studied and documented. However there is a lack of detailed investigation on the optical properties of ZrO_2, particularly a clear explanation for the luminescent mechanisms in ZrO_2 [7]. The mono phase tetragonal ZrO_2 nanoparticles were synthesized by microwave irradiation method. They exhibited sharp emission peaks at 402, 420 and 459 nm under 254 nm excitation wavelength and a broad emission band centered at 608 nm under 412 nm excitation wavelength [8]. Monoclinic and tetragonal ZrO_2 nanoparticles were synthesized by a two – phase method. They exhibited a broad emission band centered at 365 nm under 250 nm UV excitation wavelength [9]. In these cases, the luminescence intensity of ZrO_2 nanoparticles found to be very weak, and no detailed luminescence mechanisms were discussed. Further it is found that the luminescent properties of ZrO_2 depend strongly on the preparation methods. Hence, it would be of great curiosity and importance to synthesize nanocrystalline ZrO_2 by other methods and investigate their luminescence properties together with their mechanisms, to observe if some novel and strong and useful luminescence can be obtained from the nanocrystalline ZrO_2.

In the present paper, nanocrystalline ZrO_2 synthesized by reactive plasma processing is investigated for luminescence properties. As annealing process results phase transitions, changes in defect levels and elimination of non-radiative combination centers, the as synthesized ZrO_2 powder is annealed to different temperatures and times and under different atmospheres to investigate the temperature dependent luminescence behavior. Reactive plasma processing (RPP) is a novel technique, which takes advantage of the high temperature and high enthalpy of the thermal plasma jet to effect 'in-flight' chemical reactions in the presence of a reactive gas to synthesize nano-sized powders of advanced ceramics, novel coatings and convert minerals and industrial wastes to value-added materials [10].

2. Experimental techniques

3.

3.1 Synthesis of nano ZrO_2 by reactive plasma processing

Nano-crystalline powder of ZrO_2 was synthesized by reactive plasma synthesis. ZrH_2 powder, 99.9% pure from CERAC, USA was used as the precursor material. ZrH_2 powder (38–53 m size) was injected into the plasma jet using argon as the carrier gas. Oxygen gas was introduced 10mm downstream of the exit of the plasma torch. ZrH_2 dissociates to form Zr particles and hydrogen gas in the plasma jet that are subsequently converted to ZrO_2 and water vapour, which escapes along with the exhaust gas stream. Experimental set up and process details are described elsewhere [10].

2.2 Annealing of ZrO_2 nano powder

To understand the annealing temperature effect on phase structure and optical properties of ZrO_2 nano powder, the sample was annealed to 300, 600, 700, 800, 900 and 1000°C for 2 hours. It was also annealed 600°C for 3 at 1200°C for 2 hours in oxygen atmosphere. In order to know the annealing time response, the ZrO_2 sample has also been annealed at 600°C for 5, 10 and 15 hours. To know the effect of annealing time and annealing atmosphere the sample was annealed at hour and 6 hour in the presence of air, oxygen, argon and nitrogen. For each annealing experiment 0.5 g of the sample was taken in an alumina boat and annealed using a programmable tubular furnace.

2.3 Characterization of ZrO_2 nano powder

X-ray diffraction (XRD) patterns were recorded using a Bruker D8 Advance diffractometer equipped with Ni filter and operated at 40 kV, 30 mA (Cu $K\alpha_1$ radiation). . Particle size and morphology of the samples were carried out using JEOL transmission electron microscope (JEM 2100F, Japan) operated at 200 KV.For optical absorption and photoluminescence measurement, the powder samples were dispersed in ethanol with the help of ultrasonic treatment. UV–visible spectra were recorded with a spectrophotometer (Hitachi, U-3410). Photoluminescence (PL) spectra were collected using a Hitachi F-4500 fluorescence spectrophotometer (resolution, 0.2 nm) equipped with a 150 W Xe lamp as the excitation source.

4. Results and Discussion

4.1 Phase and microstructure

Figure 1 shows the x-ray diffraction pattern of ZrO_2 sample (synthesized at 16 kW) collected from the plasma reactor. The diffraction pattern shows that the synthesized powder is a mixture of monoclinic and tetragonal phase corresponding to JCPDS files 37-1484 and 79-1771 respectively [11]. The crystallite size is determined using Scherrer's formula and is found to be 25 nm and 15 nm for monoclinic and tetragonal phases.

Transmission electron microscopic image of the as-synthesized powder is shown in Fig. 2. It is clear from the figure that the powder consists of nano-sized particles, whose size ranged from about 3 nm–33 nm. Individual particles are well resolved and their spherical morphology is evident from the figure. It is seen from particle size distribution that more than 90% of the particles are below 25 nm. However, a very small fraction of particles are found to have size below 4 nm and above 30 nm.

4.2 Annealing Experiments

Figure 3 shows the X- ray diffraction patterns of the as-synthesized ZrO_2 and the sample annealed at different temperatures for 2 hours. As the annealing temperature increases, the intensity of tetragonal peak decreases, continuously, up to 900°C. At 1000°C, intensity of tetragonal peak disappears and the sample becomes completely monoclinic. The sample annealed at 1200°C in O_2 atmosphere has sharp diffraction peaks which show highly crystalline monoclinic ZrO_2.

The growth of crystallite size of the annealed samples has been calculated and displayed in table 1. It is found that with increasing annealing temperature crystallite size of tetragonal phase increases and reaches a maximum size of 29 nm at 900°C. The crystallite size of monoclinic phase also increases with increasing annealing temperature and reaches a size of 142 nm at 1200°C.

Figure 4 shows the X-ray diffraction patterns of as-synthesized ZrO_2 and the sample annealed at 600°C for 2, 5, 10 and 15 hours. From the figure it can be seen that as annealing time increases the intensity of tetragonal phase decreases gradually while that of monoclinic phase increases. Crystallite size of these samples have been calculated and displayed in table 2.

Figure 5 shows the X-ray diffraction patterns of ZrO_2 annealed at 600°C for 3 hr in Ar, N_2, air and O_2 atmospheres. XRD patterns of samples annealed in Ar and N_2 do not show much variation. But samples annealed in air and O_2 atmosphere show slight increase in the intensities of monoclinic peak.

Figure 6 shows the X-ray diffraction patterns of ZrO_2 annealed at 600°C for 6 hr in Ar, N_2, air and O_2 atmospheres. XRD patterns of samples annealed in Ar and N_2 appear same. But samples annealed in air and O_2 atmosphere have slightly increased intensities of monoclinic peak.

4.3 UV– visible absorption studies

Figure 7 shows the UV–visible absorption spectrum of reactive plasma synthesized nano ZrO_2 in the wavelength region 250–400 nm. The spectrum shows two absorption peaks at 275 nm (4.5 eV) and 314 nm (3.94 eV) corresponding to the

decrease in the value of the band gap of both tetragonal (5.7 eV) and monoclinic (5.8 eV) phase [12]. Zirconia belongs to the class of photo-resistant metal oxides and, typical of this class, new defect centers are formed by trapping of carriers by existing defects in the structure [13]. Hence, the absorption recorded on our samples should be ascribed to the formation of defects (colour centers). In general, the principal intrinsic defects in powdered zirconia are oxygen vacancies. In our samples, which contain no stabilizers, the high surface /volume ratio may favour the formation of defects, such as oxygen vacancies, leading to absorption at lower energies (donor levels located inside the forbidden band). This suggested that the redshift of the absorption peak could be due to oxygen vacancies.

To know the effect of oxygen vacancies responsible for lowering the band gap energy, the as synthesized ZrO_2 sample was annealed in the temperature range 300 –1200°C for 2 hours. Figure 7 shows the UV– visible absorption spectrum of the sample annealed at different temperatures. As temperature increases from 300°C, the 314 nm peak decreases gradually and disappears at 900°C. But the 275 nm peak gradually blueshifts up to the annealing temperature of 900°C compared to the as synthesized sample. These results suggest that although incorporation of oxygen into the structure decreases the oxygen vacancy sites, a few vacancy sites still exist up to that temperature. The sample annealed at 1200°C in oxygen atmosphere shows an absorption peak around 232 nm (5.3 eV) which corresponds to the band gap value (5.8 eV) of bulk monoclinic ZrO_2.

Figure 8 shows the UV– visible absorption spectrum of the ZrO_2 sample annealed at 600°C for 2, 5, 10 and 15 h. As the annealing time increases from 2 h, the absorption peak at 314 nm decreases and disappears for the annealing time of 10 h. While the 275 nm peak blueshifts to 235 nm for the annealing time of 15 h. These results suggest that both with increasing annealing temperature and time incorporation of oxygen into the ZrO_2 structure decreases the oxygen vacancy sites which result in the disappearance of 314 nm peak and shift of 275 nm peak to lower wavelengths.

3.4 Photoluminescence studies

Photoluminescence spectra were measured with excitation wavelength 245 nm. Figure 9 shows the photoluminescence spectra of ZrO_2 nanoparticles under 245 nm excitation in the wavelength range 250 -600 nm. Two luminescence bands centered at 325 nm and 470 nm are observed. Annealing temperature effect on photoluminescence of the sample has been investigated for different temperatures for 2 h in the wavelength range 250 - 600 nm and is shown in figure 9. Samples were excited with 245 nm. With increasing annealing temperature the PL intensity of 325 nm band increases and reaches a maximum at 700°C and then decreases and disappears for the sample annealed at 1200°C in the presence of oxygen. Conversely, the band at 470 nm decreases rapidly with increasing temperature. When annealing temperature becomes 800°C, the emission peak at 470 nm disappears.

Figure 10 presents the PL spectra of the ZrO_2 sample annealed for different times at 600°C in the wavelength range of 250–600 nm. With the increase annealing time, the emission intensity of the 325 nm band increases first, reaches a maximum when the annealing time is 5 h , and then decreases sharply (for 10 and 15 h curves), while the emission intensity of the 470 nm band decreases continuously.

Annealing atmosphere dependence on photoluminescence of the ZrO_2 sample has been investigated for nitrogen, argon, oxygen and air atmospheres. Figures 11 and 12 show the PL spectrum of the sample annealed at 600°C for 3h and 6 h in the wavelength range 250 - 600 nm. For 3 h annealing time, the intensity of 470 nm band is maximum for nitrogen and minimum for oxygen, while the intensity of 470 nm band of argon is close to that of nitrogen. For this annealing time, intensity of 325 nm band is maximum for oxygen and minimum for argon.

As the annealing time increases to 6 h, the intensity of 470 nm band disappears for oxygen and air atmosphere, while that of nitrogen and argon remains almost same. The intensity of 325 nm band of oxygen and air annealed samples decreases compared to that of 3 h annealed samples. Conversely, samples annealed in argon and nitrogen atmospheres do not show much variation for 3 h and 6 h annealing times.

So far, luminescence mechanisms of ZrO_2 are not clear and two kinds of different mechanisms have been proposed to explain luminescence [14–17]: an impurity luminescence center model and a structure-defect model. The impurity luminescence center model ascribes the luminescence of ZrO_2 to small amount of Ti^{4+} or phosphorous- -group impurity in ZrO_2. However, ZrO_2 powders herein are synthesized under the conditions free of any Ti^{4+} or phosphorous-group of elements. The structure-defect model proposes that the luminescence of ZrO_2 comes from singly ionized oxygen-vacancy defects (F^+ centers). This luminescence includes the following process: ionization, migration, recombination, and emission. Excitation using photons or electrons with energy exceeding the zirconia band gap produces electron-hole pairs. Electrons are trapped very quickly by the oxygen vacancies (V_O), creating F^+ centers. Recombination of the holes with the F^+ centers creates the excited states of the emitter $(V_O)^*$. These excited emitters undergo radiative transitions to the ground state. The recombination process can be described as follows:

$$ZrO_2 + h\gamma \rightarrow e^- + h^+ \quad (1)$$
$$V_o + e^- \rightarrow F^+ \quad (2)$$
$$F^+ + h^+ \rightarrow (V_o)^* \rightarrow V_o + h\gamma \quad (3)$$

The UV emission (325 nm) intensity of the sample has the following dependent behavior on annealing atmospheres. The UV (325 nm) emission of the sample annealed in a nitrogen atmosphere is the most intense and the UV emission of the sample annealed in an oxygen atmosphere is the weakest, but all the samples exhibit similar UV emission profiles with prominent peaks at 325 nm (Fig. 11). Therefore, we assume that the UV band of ZrO_2 nanopowders still originates from F^+ centers [18]. Although the blue emission in the wavelength range of 440–500 nm for bulk ZrO_2 was usually reported, there are a few reports dealing with the emission in the same region for nanosized ZrO_2. Petrik et al. found that the association of F^+ centers with one or two Y^{3+} ions in yttria stabilized cubic ZrO2 crystals would result in a red shift of the emission band of F^+ centers [19]. Similarly, it is expected that the association of two or more than two oxygen-vacancy defects will also lower the emission energy in comparison with F^+ centers. This situation is analogous to the emission property of exciton molecules in that they have lower emission energy than free excitons [20]. In addition, reducing environment of the process leads to the existence of large amounts of oxygen-vacancy defects in ZrO_2 nanopowders. This also provides the opportunity for the association among oxygen vacancy defects. Therefore, it is reasonable to assume that the 470 nm band with lower emission energy arises from the singly ionized associated oxygen vacancy defects (AOD^+ centers) (i.e. singly ionized two-oxygen-vacancy-defect associations: $(F–F)^+$).

If the 325 nm band and the 470 nm band come from F^+ centers and AOD^+ centers, respectively, it is not surprising that the PL spectra have such changing behaviors with annealing time and temperature (Fig. 9 and 10). With the increase of annealing time, the concentration of AOD^+ centers decreases continuously due to the diffusion of the oxygen in the air into ZrO_2 particles and the dissociation of AOD^+ centers into F^+ centers. Therefore, the emission intensity of the 470 nm band exhibits a continuous decrease with the increase of annealing time. There are several factors that affect the concentration of F^+ centers. One factor is the transformation from AOD^+ centers to F^+ centers mentioned above, which will lead to the increase of the concentration of F^+ centers. The other factors are the oxygen diffusion from the air into ZrO_2 particles, the decrease of surface area owing to the enlarged particle sizes, etc., which will result in the decrease of the concentration of F^+ centers. At the beginning, the former factor dominates, and then the concentration of F^+ centers increases. Thus, the emission intensity of the 325 nm band presents an enhancement with the increase of annealing time. With further increase in annealing time, the latter factors dominate and the concentration of F^+ centers will decrease. This is why the emission intensity of the 325 nm band subsequently decreases with increasing time (10 h, 15 h in Fig. 10).

4. Conclusion

Nanocrystalline ZrO_2 sample synthesized by reactive plasma processing has been annealed to different temperatures (300 - 1200°C), for different times (2 – 15 h) and at different atmospheres (Ar, N_2, O_2 and air) to investigate its UV – visible absorption and photoluminescence characteristics. UV – visible absorption studies demonstrated two absorption bands at 3.94 and 4.5 eV which are lower than the band gap of ZrO_2. This narrowing of band gap was attributed to the oxygen vacancy levels developed in the band gap ZrO_2.This was demonstrated by annealing experiments where at 1200°C, 4.5 eV band was blue shifted to 5.3 eV which is close to band gap of monoclinic ZrO_2 (5.8 eV).

Photoluminescence spectra of ZrO_2 sample showed two emission bands at 325 and 470 nm. According to the emission-intensity dependence on the annealing atmospheres, it was proposed that the 325 nm band and the 470 nm band originate from F^+ centers and AOD^+ centers, respectively. The changing behaviors of the emission intensities for both the 325 nm band and the 470 nm band with the annealing conditions, such as annealing time and annealing temperature, are interpreted by the dependence of the concentrations for F^+ centers and AOD^+ centers on the annealing conditions.

References

[1] D.G. Shchukin, and R.A. Caruso, Adv. Funct. Mater. 13, 789 (2003)
[2] H. Althues and S. Kaskel, Langmuir 18, 7428 (2002)
[3] A. Caballero, J.J. Morales, A.M. Cordon, J.P. Holgado, J.P. Espinos and A.R. Gonzales-Elipe, J. Catal. 235, 295 (2005)
[4] E.C. Subbarao and H.S. Maiti, Adv. Ceram. 24, 731 (1988)
[5] G.D. Wilk and R.M. Wallace, Appl. Phys. Lett. 112, 76 (2000)
[6] S. Shukla, S. Seal, R. Vij, S. Bandyopadhyay, *Nano Lett. 3*, 397 (2003)
[7] V. Chernov, A. Belykh, R. Melendrez, M. Barboza-Flores, *J. Non-Cryst. Solids 352*, 2543 (2006)
[8] J. Liang, Z. Deng, X. Jiang, F. Li, Y. Li, *Inorg.Chem. 41*, 3602 (2002)
[9] N. Zhao, D. Pan, W. Nie, X. Ji, *J. Am. Chem. Soc. 128*, 10118 (2006)

[10] S. Jayakumar, P.V. Ananthapadmanabhan, K. Perumal, T.K. Thiyagarajan, S.C. Mishra, L.T. Su, A.I.Y. Tok, J. Guo, Mater. Sci. Eng., B 176, 894 (2011).
[11] S.Jayakumar, P.V. Ananthapadmanabhan, K. Perumal, T. K. Thiyagarajan, S.C, Mishra, G. Suresh, L.T. Su, A.I.Y . Tok, J.Guo Materials Chemistry and Physics. 140, 176 (2013)
[12] R.H. French and S.J. Glass, Physical Review B, 498, 5133 (1994).
[13] A. Emeline, G. V. Kataeva, and A.S. Litke, Langmuir 14 5011 (1998).
[14] P. Iacconi, D. Lapraz, R. Caruba: Phys. Status Solidi A 50, 275 (1978).
[15] M. Garc´ıa-Hip´olito, R. Mart´ınez, O. Alvarez-Fregoso, J. Luminesc. 93,9 (2001).
[16] V.A. Emeline, N. Serpone, Chem. Phys. Lett. 345,105 (2001).
[17] W.C. Hsieh, C.S. Su, J. Phys. D: Appl. Phys. 27, 1763 (1994).
[18] A. Emeline, G.V. Kataeva, A.S. Litke, Langmuir 14,5011 (1998).
[19]22 N.G. Petrik, D.P. Taylor, T.M. Orlando, J. Appl. Phys. 85, 6770 (1999).
[20] E.I. Rashba and M.D. Sturge, Editor, *Excitons*, North-Holland, Amsterdam, New York, Oxford (1982)

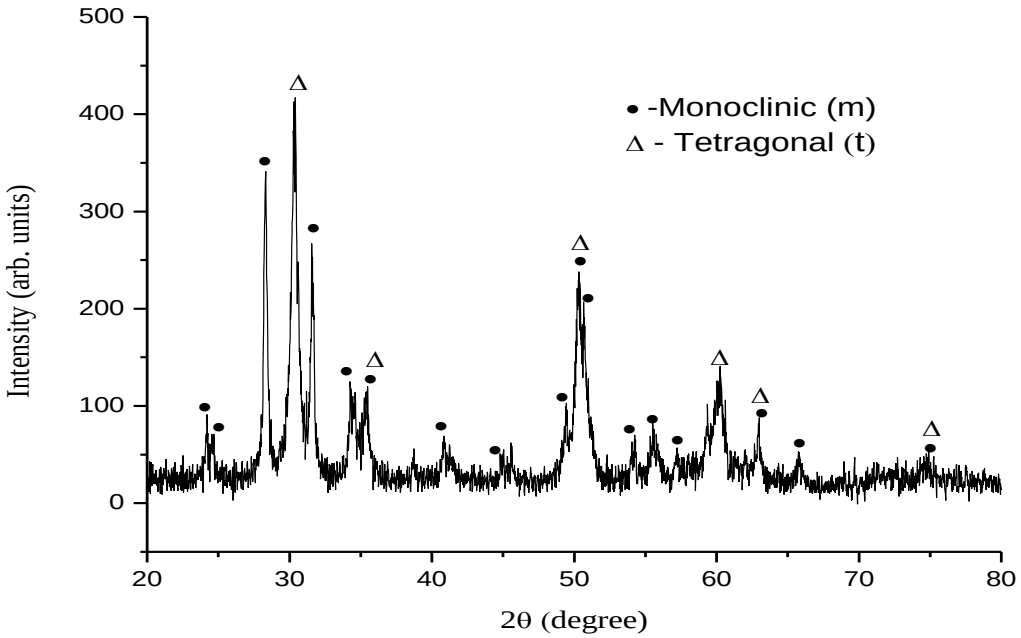

S.Jayakumar, Photoluminescence of Reactive Plasma Synthesized ZrO_2 Nanoparticles, Figure 1 X-ray diffraction pattern of plasma synthesized ZrO_2 powder

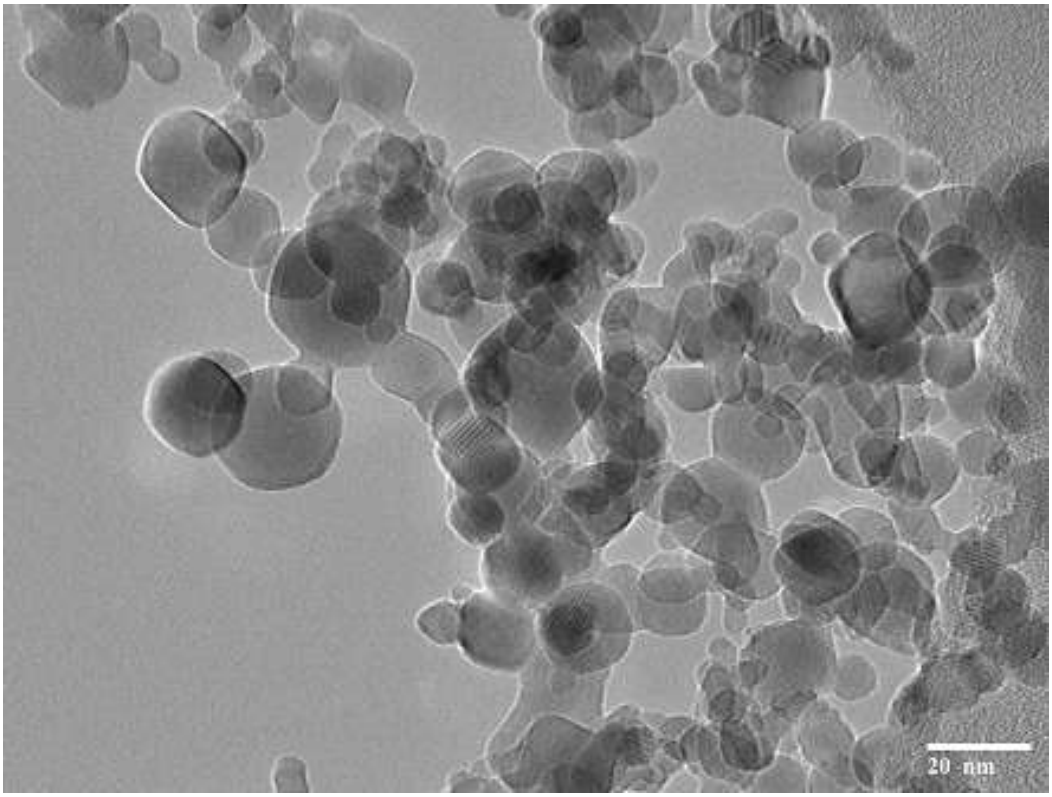

S.Jayakumar, Photoluminescence of Reactive Plasma Synthesized ZrO_2 Nanoparticles, Figure 2 TEM micrograph of plasma synthesized ZrO_2 powder

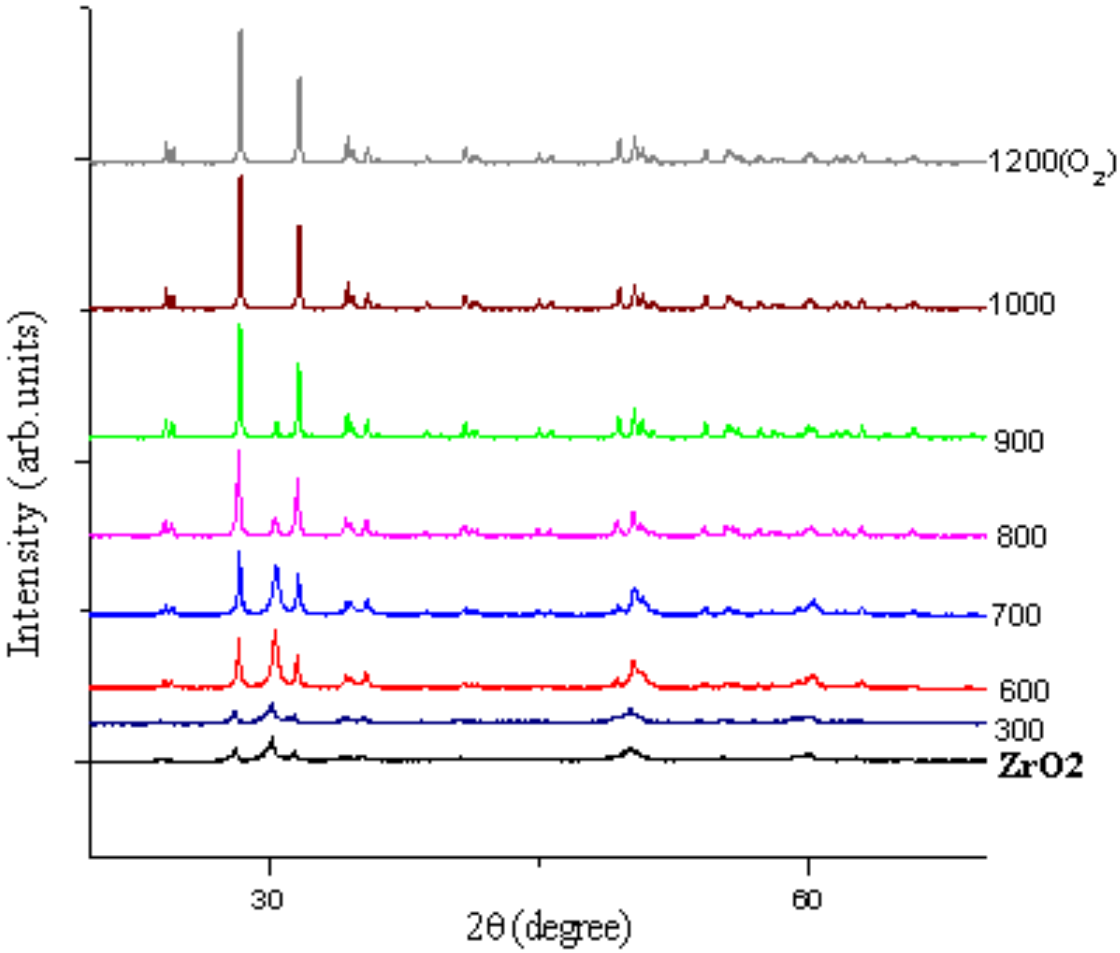

S.Jayakumar, Photoluminescence of Reactive Plasma Synthesized ZrO_2 Nanoparticles, Figure 3 X-ray diffraction patterns of as-synthesized ZrO_2 annealed at different temperatures for 2 hours

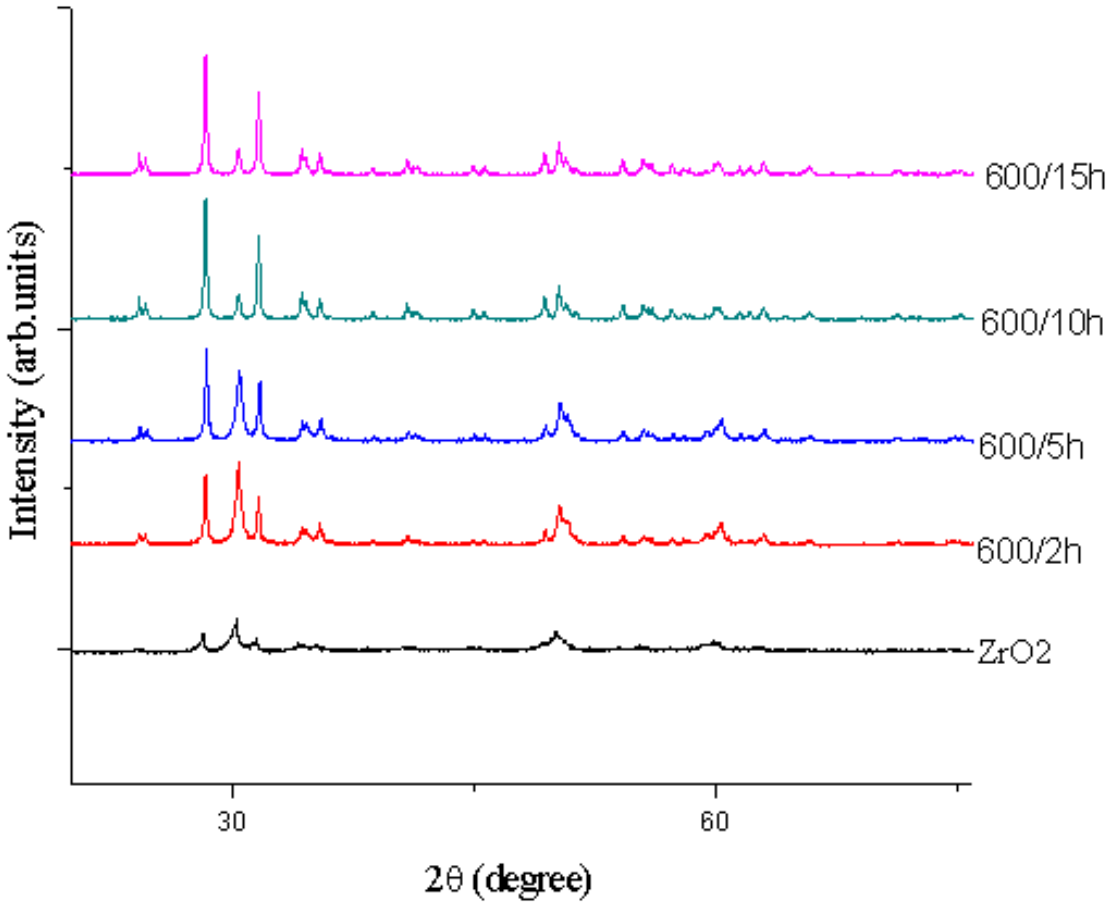

S.Jayakumar, Photoluminescence of Reactive Plasma Synthesized ZrO_2 Nanoparticles, Figure 4 X-ray diffraction patterns of as-synthesized sample C and sample c annealed at 600°C for 2, 5, 10 and 15 hours

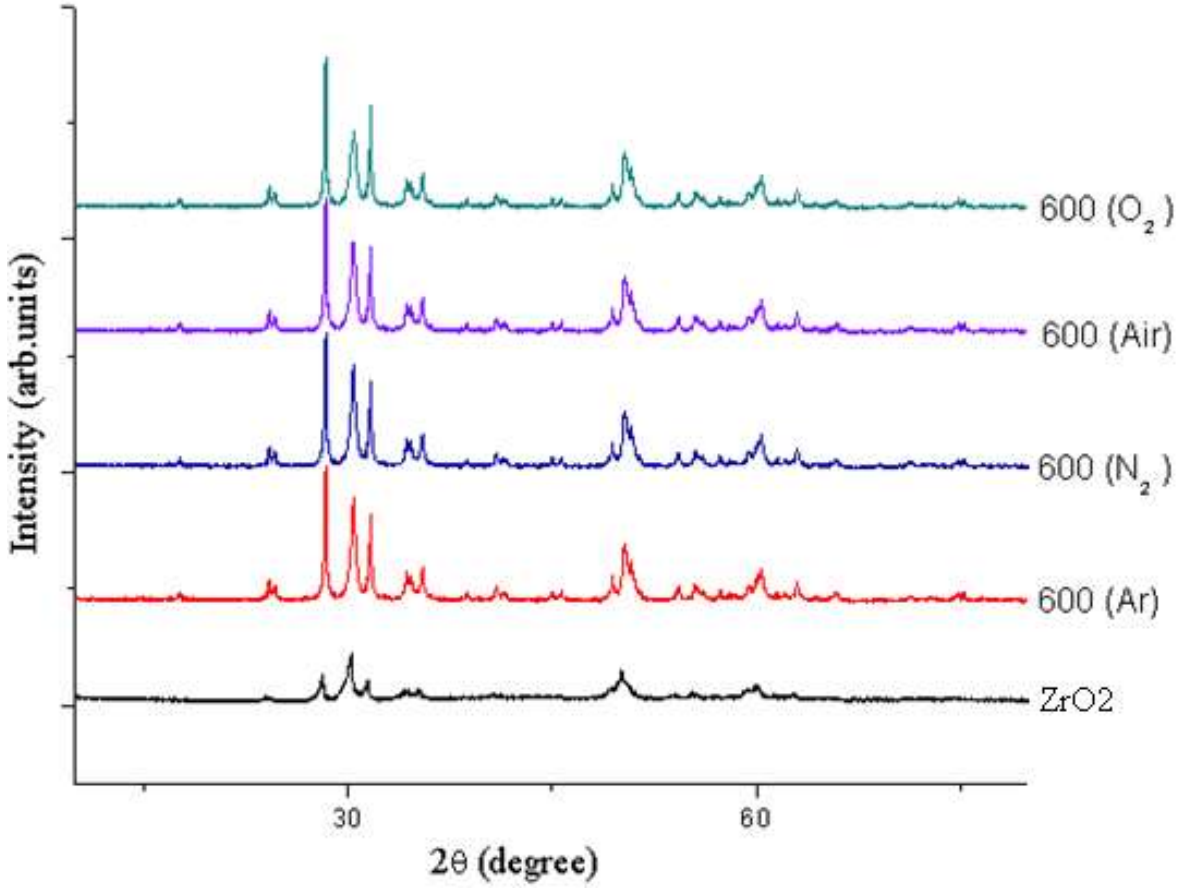

S.Jayakumar, Photoluminescence of Reactive Plasma Synthesized ZrO_2 Nanoparticles, Figure 5 X-ray diffraction patterns of ZrO_2 annealed at 600°C for 3 hours in Ar, N_2, air and O_2 atmosphere

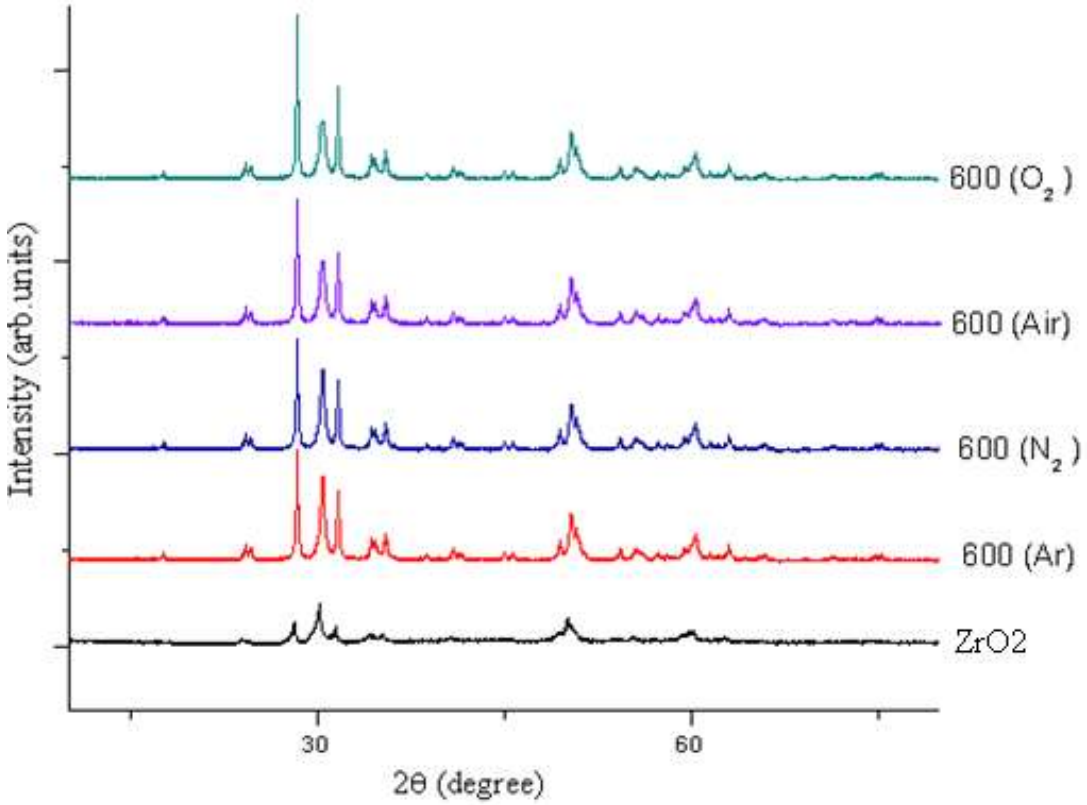

S.Jayakumar, Photoluminescence of Reactive Plasma Synthesized ZrO_2 Nanoparticles, Figure 6 X-ray diffraction patterns of ZrO_2 annealed at 600°C for 6 hours in Ar, N_2, air and O_2 atmosphere

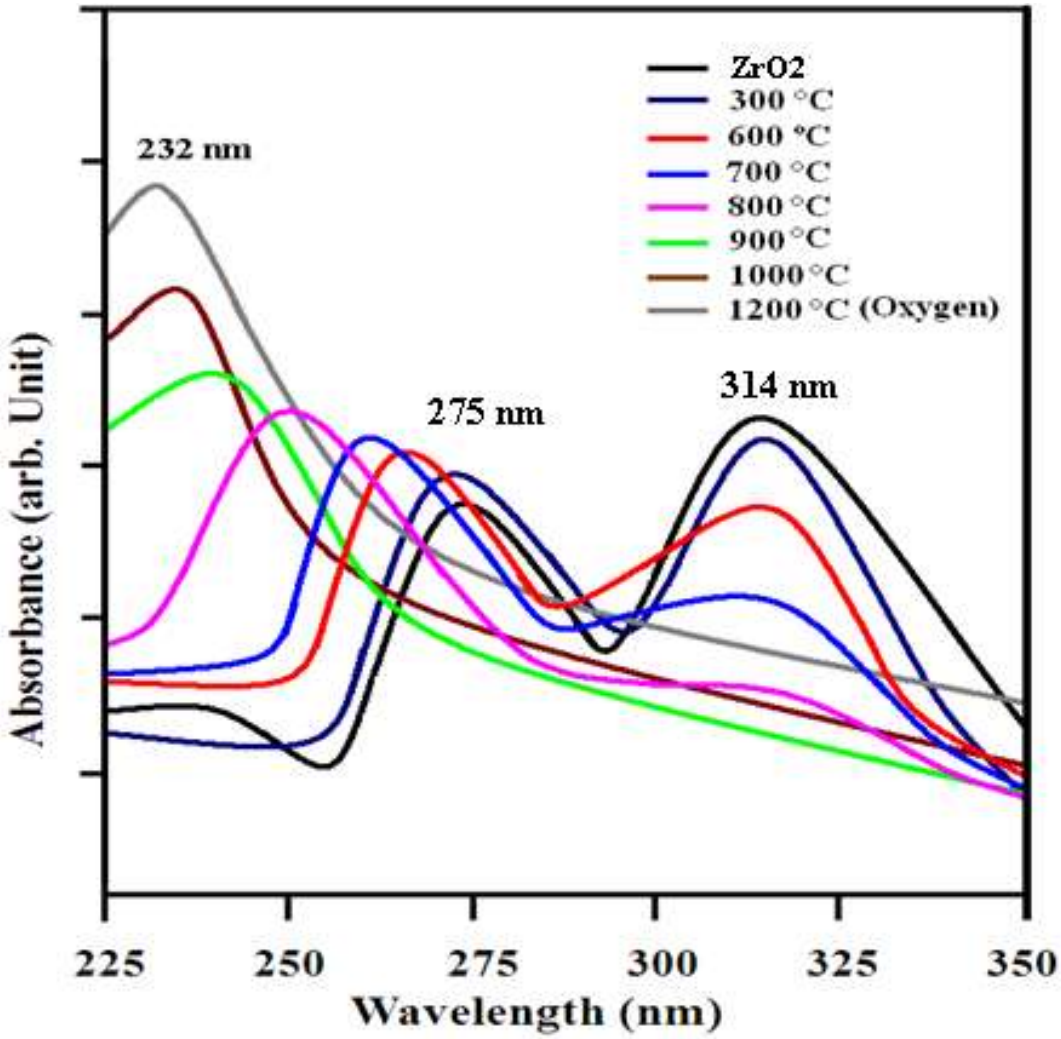

S.Jayakumar, Photoluminescence of Reactive Plasma Synthesized ZrO_2 Nanoparticles, Figure 7 UV– visible absorption spectrum of ZrO_2 annealed at different temperatures for 2 h

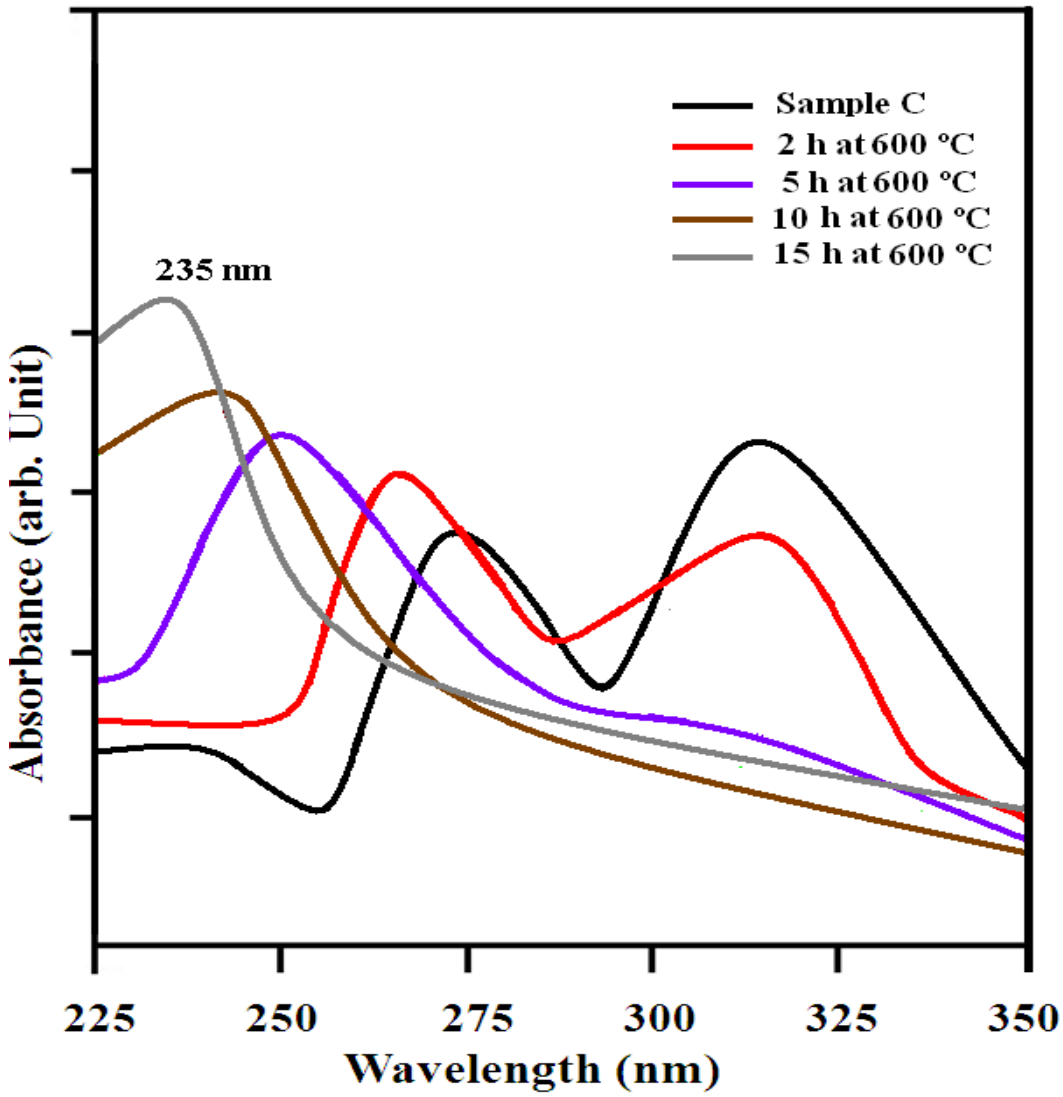

S.Jayakumar, Photoluminescence of Reactive Plasma Synthesized ZrO_2 Nanoparticles, Figure 8 UV– visible absorption spectrum of ZrO_2 annealed at 600°C for 2, 5, 10 and 15 h

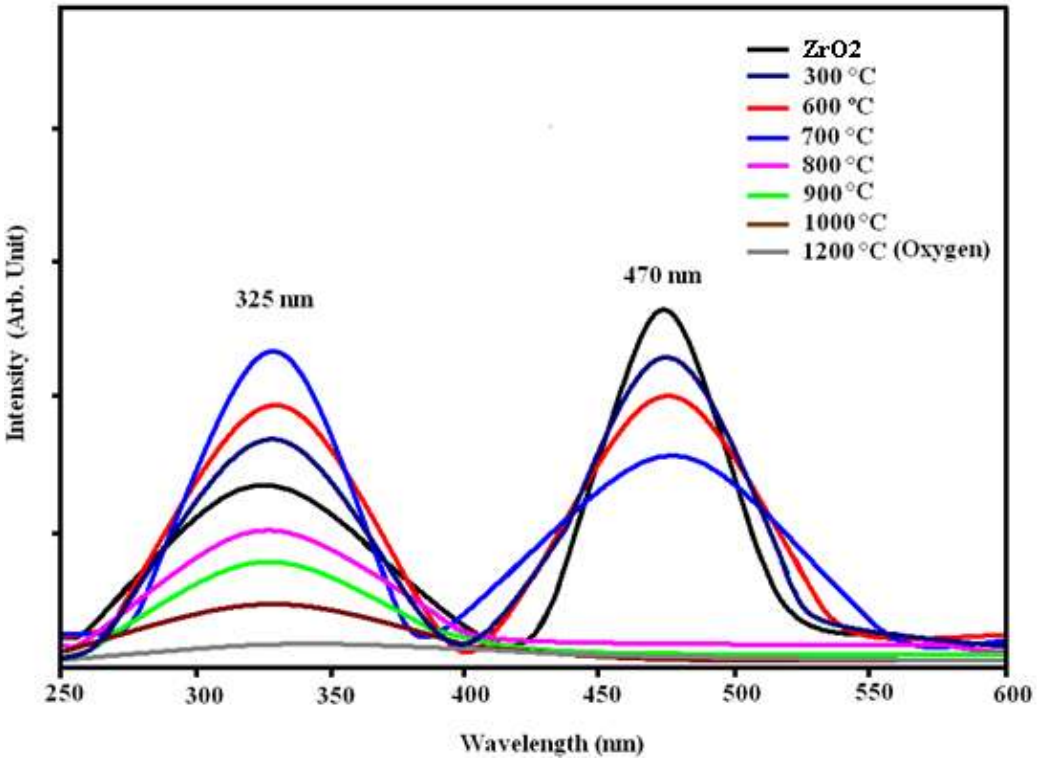

S.Jayakumar, Photoluminescence of Reactive Plasma Synthesized ZrO_2 Nanoparticles, Figure 9 PL spectra of ZrO_2 sample annealed for different temperatures (λ_{ex} = 245 nm)

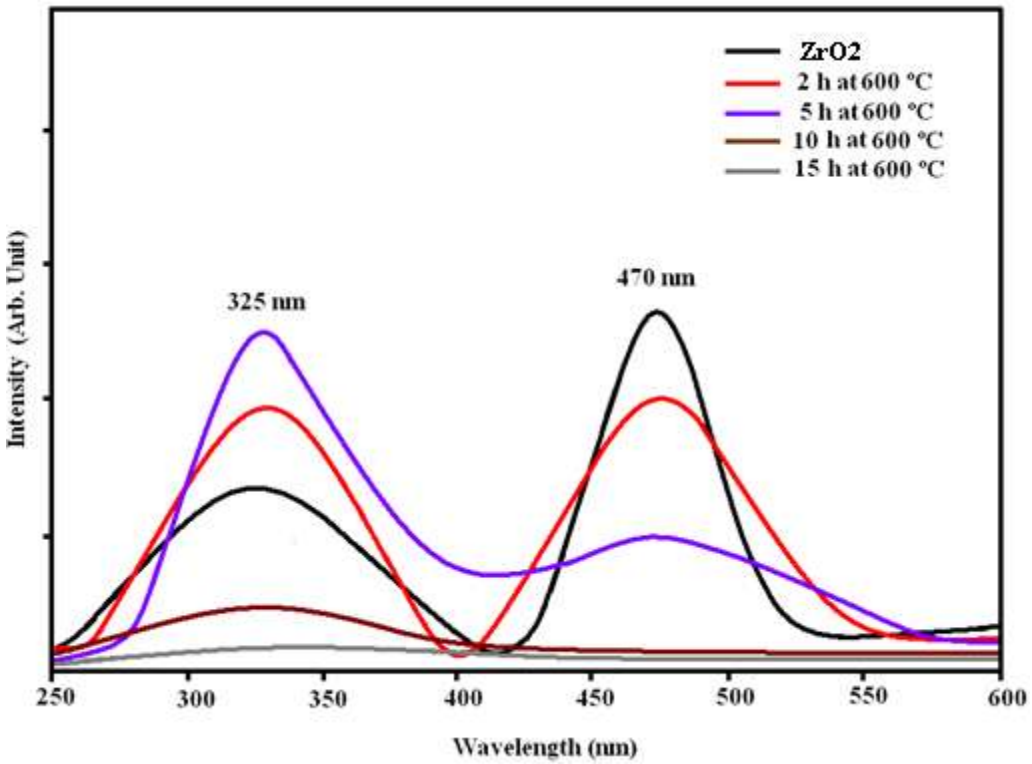

S.Jayakumar, Photoluminescence of Reactive Plasma Synthesized ZrO_2 Nanoparticles, Figure 10 PL spectra of ZrO_2 annealed for different times at 600°C (λ_{ex} = 245 nm)

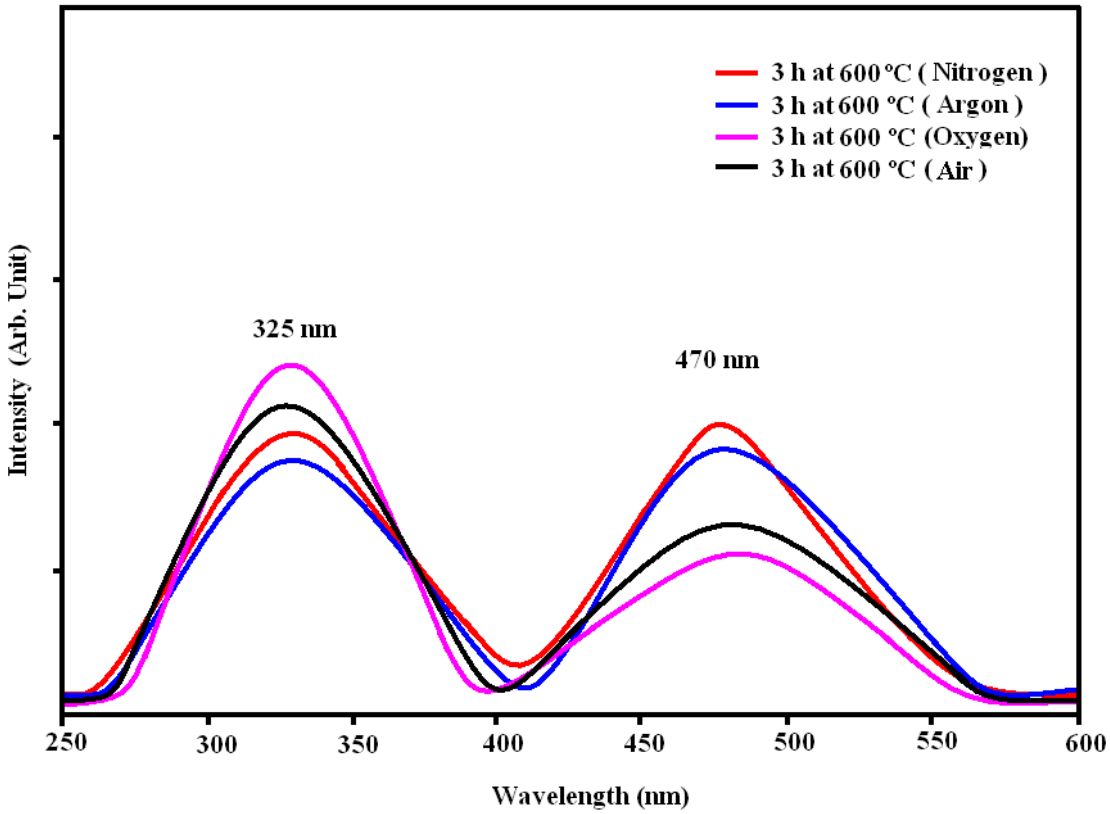

S.Jayakumar, Photoluminescence of Reactive Plasma Synthesized ZrO_2 Nanoparticles, Figure 11 PL spectra of ZrO_2 annealed at 600°C for 3h in N_2,Ar,O_2 and air (λ_{ex} = 245 nm)

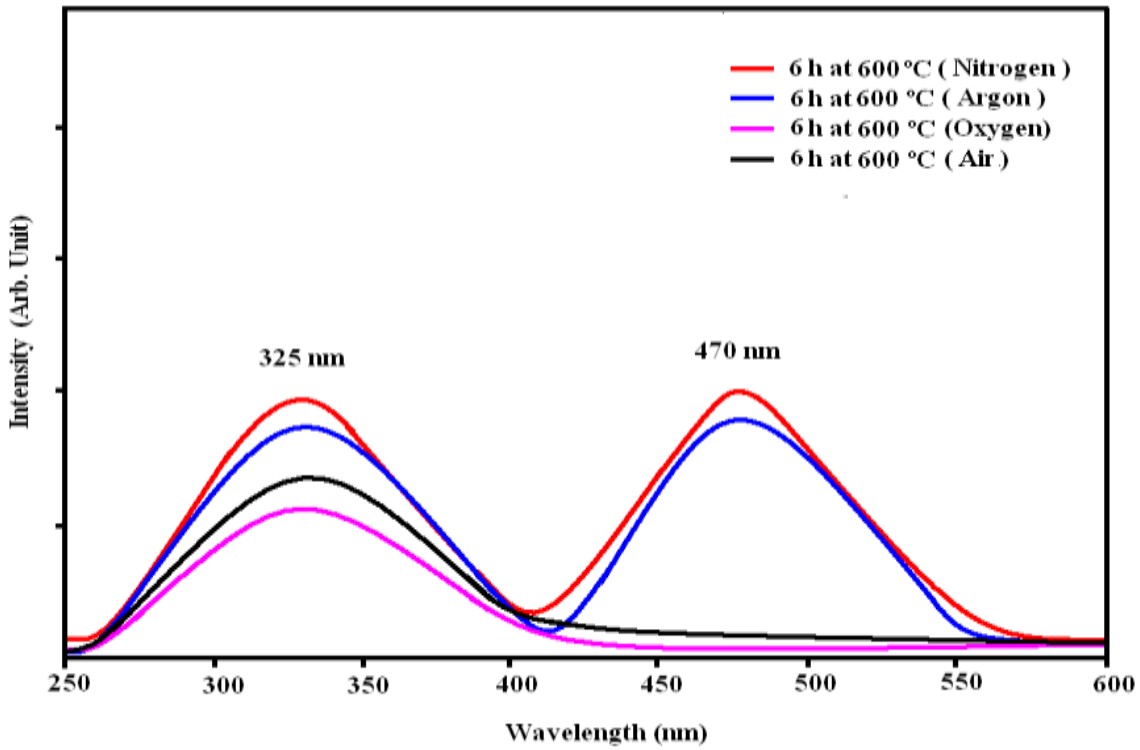

S.Jayakumar, Photoluminescence of Reactive Plasma Synthesized ZrO_2 Nanoparticles, Figure 12 PL spectra of ZrO_2 annealed at 600°C for 6h in N_2,Ar,O_2 and air (λ_{ex} = 245 nm)

Table 1 Crystallite size of sample C annealed at different temperatures for 2 hours

S.No	Sample Annealing history	Monoclionic	Tetragonal
		Crystallite size (nm)	Crystallite size (nm)
1	As-synthesized ZrO_2	25	15
2	300°C /2 h	33	18
3	600°C /2 h	45	22
4	700°C /2 h	64	24
5	800°C /2 h	87	27
6	900°C /2 h	102	29
7	1000°C /2 h	126	-
8	1200°C /2 h	142	-

Table 2 Crystallite size of sample C annealed at 600°C for 2, 5, 10 and 15 hours

S.No	Sample Annealing history	Monoclionic	Tetragonal
		Size (nm)	Size (nm)
1	As-synthesized ZrO_2	25	15
2	600°C /2 h	45	22
3	600°C /5 h	53	23
4	600°C /10 h	71	25
5	600°C /15 h	84	26

